Usage of *Grewia bicolor* Juss leaves extract as green corrosion inhibitor for Steel XC40 in sulfuric acid medium

M.O. Sidine,[1] H. Lahbib,[2] A. Hadou,[1] M. Ba,[3] M. Benmessaoud,[4] Y. Ben Amor[2] and B. Ould Elemine[1]*

[1]*Unité de Chimie Moléculaire et Environnement, Département de Chimie, FST, UN, Nouakchott, Mauritanie*
[2]*Research Laboratory of Environmental Sciences & Technologies, Higher Institute of Environmental Sciences and Technology, Carthage University, Ben Arous, Tunisia*
[3]*Unité de Recherche: Electrochimie, matériaux et environnement (UREME), UR17ES45, Faculté des Sciences de Gabès, Cité Erriadh, 6072 Gabes, Tunisia*
[4]*Energy, Materials and Sustainable Development Team CERNE2D, Higher School of Technology Salé, Mohammed V University in Rabat 8007, Morocco*
**E-mail: ouldeleminebrahim2009@gmail.com*

Abstract

The inhibitive effect of a methanol extract of *Grewia bicolor* Juss (Gbj) leaves on the corrosion of XC48 steel in 0.5 M H_2SO_4 solution has been evaluated by weight loss measurement as well as potentiodynamic polarization (PDP), electrochemical impedance spectroscopy (EIS) and surface characterization techniques. The presence of this extract brings down remarkably the corrosion rate of XC48 steel in 0.5 M H_2SO_4 solution. The results from this corrosion test clearly showed that the extract behaves as a mixed type corrosion inhibitor with the highest inhibition at 1500 ppm. The effect of temperature on the corrosion behavior of XC48 steel was studied in the range of 298–333 K. The activation and free energy values of the inhibition reaction support the hypothesis of a/the physisorption mechanism well described by the Langmuir equilibrium mode. Scanning electron microscopic (SEM) observations showed that the Gbj extract forms a protective layer over the metallic surface that isolates the metal from aggressive acid solution and protects it against corrosive dissolution. Finally, results of FTIR analysis indicate that the important role played by the oxygen atoms and aromatic rings in the process of adsorption.

Received: October 31, 2022. Published: July 27, 2023 doi: 10.17675/2305-6894-2023-12-3-10

***Keywords**: methanol extract of Grewia bicolor Juss, XC48 steel, corrosion inhibition.*

1. Introduction

Sulfuric and hydrochloric acids are throughout used in industries for different treatment such as acid pickling process for taking off the oxides and other contaminants from the metal surface. However, due to the aggressiveness of acids for plain carbon steels and ferrous alloys, corrosion can be reduced by adding corrosion inhibitors in small concentrations [1–3]. On the other hand, stainless steel is employed in different industries although it suffers from

some type of corrosion in different environments [4–6]. In order to protect the metal surface from these aggressive environments, several techniques such as coatings, cathodic protection, anodic protection and corrosion inhibitors are available. In many practical applications, the use of corrosion inhibitors is the most widely used method for corrosion mitigation. The mechanism of corrosion inhibition by organic substances relies on the fact that the chemical compounds are adsorbed on the surface of metals through interactions with their adsorption centers which are the conjugated double bounds, aromatic rings or heteroatoms [7] which defines the corrosion inhibition efficiency [8–11]. Despite their high effectiveness, most commonly used inhibitors are likely to be a source of environmental degradation prompting scientists to prospect a wide range of new green inhibitors [12–16]. In the literature, the use of natural products as corrosion inhibitors dates back to the 1930 [17]. In the last decade, the treatment of mild steel corrosion in acidic solutions by various types of plant extracts has been studied with attention, given the increasing demand for green chemistry in the industrial sector. Plant extracts have indeed a high efficiency of corrosion inhibition [18–20], and low environmental risk. They are also inexpensive, readily available and renewable [21–23]. Several studies on the corrosion-inhibiting performance of plant extracts have been focused on mild steel and low-alloy protection under acid conditions. For instance, the influence of *Citrus aurantium* leaves extracts on mild steel corrosion in 1 M H_2SO_4 was studied by Karim H. Hassan *et al.* [24] through the effect of temperature and inhibitor concentration. Using the weight loss technique, they revealed that 10 ml/l of this leaves extract was sufficient to yield a maximum inhibition efficiency of 89% at 313 K. The adsorption isotherm study indicated an adsorption process conforming to the Langmuir isotherm model, and the mode of adsorption was physisorption. In another work on Mango (*Mangifera indica*) extract as inhibitor of corrosion phenomena affecting mild steel in 1 M H_2SO_4 by adopting thermometric, gravimetric and potentiodynamic polarization methods [25]. In this situation, the measurements were carried out at temperatures varying from 303 to 333 K. The results showed that this extract performed as a mixed-type inhibitor with a best inhibition efficiency of 74% at optima inhibitor concentration of 0.97 g/L and temperature of 305.33 K. The adsorption of the mango extract on the mild steel surface was spontaneous and proceeded according to the physical adsorption mechanism. Other results were reported by Roland Tolulope Loto [26], who investigated the inhibitory action, the combined admixture of *Rosmarinus officinalis* and zinc oxide on low carbon steel in 1 M HCl and H_2SO_4 solutions. Results suggested that the additive adsorbs on the surface of the low carbon steel according to Langmuir and Frumkin adsorption isotherms. Maximum inhibition efficiencies of 93.26% in HCl and 87.7% in H_2SO_4 acid solutions with mixed type inhibition behavior in both acids were observed. More recently, Fatima Bouhlal *et al.* [27] analyzed Coffee grounds extract as inhibitory of the corrosion of C38 steel in 1 M hydrochloric acid medium. Their results confirmed that the extract coffee ground acted as a mixed type inhibitor with an inhibitory power increasing at higher concentration. A high inhibition efficiency, equal to 97.4% was reached with 2 g/L. Furthermore, thermodynamic calculations showed physisorption molecular interaction with the steel's surface according

to Langmuir adsorption isotherms. Hana Lahbib *et al.* [28] using weight loss experiments and classical electrochemical methods and surface characterizations examined the inhibiting effect of dwarf palm and *Cynara cardunculus* leaves extract for St37 steel in 15% H_2SO_4 solution. These plant extracts acted as mixed-type inhibitors with a predominant anodic effect. The adsorption process on the metallic surface was consistent with the Langmuir adsorption isotherm, and the mode of adsorption of both extracts on the St37 steel surface was physisorption. High inhibition efficiencies of 76.13% and 69.35% were obtained with 30 ppm of dwarf palm and *Cynara cardunculus* leaves extracts, respectively. So far, no data are available on the corrosion inhibiting properties of *Grewia bicolor* Juss plant. The aim of this work was to evaluate the inhibitory action of leaves extract of the plant *Grewia bicolor* Juss against the corrosion of XC48 steel in H_2SO_4 medium (0.5 M) using weight loss method, potentiodynamic polarization and electrochemical impedance spectroscopy (EIS) methods. These measurements were supplemented by scanning electron microscopy (SEM) and Fourier-transform infrared spectroscopy (FTIR).

2. Materials and methods

2.1. Electrochemical cell

Electrochemical experiments were performed using a three-electrode cell system with a Pt mesh as auxiliary electrode, an Ag/AgCl reference electrode and a XC48 carbon steel working electrode with a geometric area of 1 cm^2. The chemical composition of the XC48 steel used was determined as (wt%): C = 0.418; M n = 0.730; Mo = 0.012; P = 0.016; S = 0.019; Si = 0.245; Ni = 0.079; F = 0.777 and Fe = 98.098 [29]. Before each experiment, the mild steel working electrode surfaces were successively cleaned with SiC abrasive papers (400, 600, 1000 and 1200 grades), washed with distilled water and finally degreased with acetone and dried at room temperature.

2.2. Solutions

The aggressive 0.5 M H_2SO_4 solution electrolyte was prepared by the dilution of an analytical grade reagent concentrated H_2SO_4 with distilled water. The inhibitor concentration was varied from 400 to 1500 ppm.

2.3. Plant extract

The leaves of *Grewia bicolour* Juss, used as a green inhibitor, were retrieved from the Kiffa, a town located in the south of Mauritania, about 600 km from the capital Nouakchott in January 2019. The extraction was carried out using the Soxhlet method as performed by Gutam *et al.* [30]. The plant was first cleaned with sterile water and dried at room temperature for 2 months. The dried leaves were then crushed into fine loose particles. The air-dried leaves (30 g) were coarsely powdered and extracted with methanol (200 ml) in Soxhlet apparatus for 8 h. The extract was filtered and concentrated under reduced pressure at 40°C using rotary evaporator to obtain a viscous semi solid mass.

2.4. Weight loss measurements

The weight loss experiments were carried out according to the standard method (ASTM, G31-72). The effect of the addition of leaves extract was investigated at different temperatures and various concentrations. Cylindrical XC48 steel specimens having dimensions of ($r = 0.975$ cm, $h = 0.77$ cm and $S = 4.713$ cm^2) were initially weighed in an electronic balance. The weighed samples were then immersed in 50 mL of 0.5 M H_2SO_4 with and without inhibitor, in the temperature range of 298–333 K over 24 hours. After immersion, the samples were taken out, cleaned with distilled water, dehydrated with acetone, dried and reweighed. To ensure the repeatability of measurements, every experiment was performed in quintuplicate and the average weight loss per gram was recorded. Values of the weight loss rate (in g/cm^{-2}·h^{-1}) and percentage protection efficiency (%) were calculated from the following two equations [31, 32]:

$$C_R = \frac{\Delta m}{A \times t} \quad (1)$$

$$IE\% = \frac{C_{R0} - C_R}{C_{R0}} \times 100 \quad (2)$$

where Δm was the specimen weight loss in g, A the specimen total surface area in cm^2 and t the immersion time in hours. C_{R0} and C_R were the weight loss rates of carbon steel in the acid medium in the absence and presence of the extract, respectively.

2.5. Electrochemical measurements

All electrochemical measurements were carried out using a VersaSTAT monitored by Versa Studio software, and were performed in acid medium with and without green inhibitor five times to ensure the reproducibility. The measurements were recorded after 1 hour of immersion at the Open Circuit Potential (OCP) for the stabilization of the system.

2.5.1. Electrochemical polarization

The Potentiodynamic polarization curves were recorded at a constant scan rate of 0.5 mV/s. The potential range was ±250 mV *versus* E_{corr}. The values of corrosion current density (I_{corr}) were estimated using the Tafel extrapolation method [5]. The inhibition efficiency (η%) was calculated using Equation (3), as follows [33, 34]:

$$\eta\% = \frac{i_{corr(uninh)} - i_{corr(inh)}}{i_{corr(uninh)}} \times 100 \quad (3)$$

where, $i_{corr(inh)}$ and $i_{corr(uninh)}$ represent the corrosion current density in the inhibited and uninhibited medium, respectively. Corrosion parameters including corrosion current density (i_{corr}), corrosion potential (E_{corr}), cathodic and anodic Tafel slopes (β_c and β_a) were evaluated by extrapolating the linear parts of cathodic and anodic Tafel curves to the point of

intersection [35]. The degree of surface coverage (θ) was calculated from the values of the inhibition efficiency, where $\theta = \frac{1}{100} \times \eta\%$ [36, 37].

2.5.2. EIS measurements

Electrochemical Impedance Spectroscopy (EIS) measurements were carried out over a frequency range of 100 kHz to 0.1 Hz with 10 points per decade; a sine wave with 10 mV amplitude was used to perturb the system. The impedance diagrams are given in the Nyquist representation. The inhibition efficiency (*IE*%) of the inhibitor has been found from the charge transfer resistance values according to the following Equation (4) [38, 39]:

$$IE_z\% = \frac{R_t^{inh} - R_t^0}{R_t^{inh}} \times 100 \quad (4)$$

where R_t^0 and R_t^{inh} are the charge transfer resistance in the corrosion medium in the absence and in the presence of the green inhibitor, respectively.

2.6. SEM Observations

The morphology of XC48 mild steel working electrode was obtained by scanning electron microscopy (SEM) and energy-dispersive X-ray (EDX) assays by using Quattro ESEM-Thermo Fisher for samples immersed in 0.5 M sulfuric acid without and with 1500 ppm of *Grewia bicolor* Juss extract inhibitor at 298 K for 24 h.

2.7. FT-IR Analysis

Infrared spectroscopy was adopted to identify the composition of both the *Grewia bicolor* Juss leaf extract and the layer formed on the surface of XC48 steel working electrode. Attenuated Total Reflectance Fourier-transform infrared spectroscopy (ATR-FTIR) analysis were carried out with a Perkin Elmer Spectrum BX using a KBr. the wavelength range was 400 cm^{-1} to 4000 cm^{-1}.

3. Results and Discussion

3.1. Weight loss measurements

3.1.1. Concentration effect

The effect of the addition of *Grewia bicolor* Juss leaves extract tested at various concentrations on XC48 steel corrosion in H_2SO_4 medium (0.5 M) was studied by using mass loss measurements at 298 K after 24 h of immersion time. The corresponding data given in Table 1 and showed that the corrosion rate was depending on the inhibitor concentrations. The rise in the extract concentration increased the inhibition efficiency by 88.63% at 1500 ppm. The inhibitory action of natural compounds against steel corrosion can be attributed to the component adsorption on the metal surface. This adsorption limited the

dissolution of metal by blocking its corrosion sites and hence decreasing the weight loss with the increasing efficiency as the concentration increases [40].

Table 1. Effect of GBS extract concentrations on corrosion data XC48 steel in 0.5 M H_2SO_4 after 24 h of immersion at 298 K.

***C* (ppm)**	**$C_R \cdot 10^3$ (g/cm^{-2}·h^{-1})**	***IE*%**
Blank	2.20	–
400	0.499	77.59
800	0.431	80.41
1000	0.294	86.64
1500	0.250	88.63

3.1.2. Effect of temperature

The effect of temperature on the inhibition efficiency and corrosion rate at optimum concentration (1500 ppm), was studied at different temperatures, ranging from 298 K to 333 K for 24 h of immersion by weight loss measurements. The corrosion rate values are summarized in Table 2. We clearly observed that raising temperature provoked an increase in steel dissolution and corrosion rates with a marked decrease in inhibition efficiencies at high temperatures. According to the literature, [41, 42] when the increase in temperature causes a decrease in the inhibition efficiency, this is possibly due to the desorption of the components of the extract on the metal surface. In this context, the adsorption is mainly due to the electrostatic interaction which decreases at high temperature [41]. This confirms that the adsorption process is chiefly physisorption type [43]. It can be seen from this table that the inhibition efficiency decreases, in opposite, the corrosion rate raises with temperature raising.

Table 2. Weight loss corrosion rate and inhibition efficiency of XC48 steel as a function of temperature in H_2SO_4 with and without Gbj extract.

Temperature (K)	**Blank**		**1500 ppm**		
	***W* (g)**	**$C_R \cdot 10^3$ (g/cm^{-2}·h^{-1})**	***W* (g)**	**$C_R \cdot 10^3$ (g/cm^{-2}·h^{-1})**	***IE*%**
298	0.2493	2.20	0.0291	0.25	88.63
308	0.5106	4.51	0.1319	1.16	74.16
318	0.7039	6.22	0.2629	2.32	62.65
313	0.8324	7.36	0.4257	3.76	48.86

3.2. Thermodynamic and activation parameters

Adsorption is an important process in corrosion inhibition as the inhibition of metal corrosion by organic molecules is often due to adsorption of the inhibitor molecules onto the metal surface thereby blocking the active sites that are subject to corrosion reaction [44]. The activation parameters associated with XC48 mild steel corrosion in 0.5 M H_2SO_4 solution without and with optimum concentration were calculated using the Arrhenius plot according to Equations (5, 6):

$$\ln(C_R) = \frac{E_a}{2.303RT} + \ln A \tag{5}$$

$$\ln\left(\frac{C_R}{T}\right) = \left(\ln\left(\frac{R}{Nh}\right) + \frac{\Delta S}{2.303R}\right) - \frac{\Delta H}{2.303RT} \tag{6}$$

where E_a is the apparent activation energy, R represents the universal gas constant, T is the absolute temperature and A is the frequency factor. In the other equation, h is Planck's constant, N is for the number of Avogadro constant, T is absolute temperature (K), ΔS represents the change in entropy of activation (J/mol·K), and ΔH is the apparent enthalpy of activation (kJ/mol) [45].The Arrhenius plots ($\ln C_R$ *vs.* $1/T$) and the transition state plots ($\ln(C_R/T)$ vs. $1/T$) for XC48 mild steel corrosion in 0.5 M H_2SO_4 without and with optimum concentration (1500 ppm) of Gbj extract are given in Figure 1 ((a) and (b) respectively). The values determined from the slopes of the straight lines obtained are cited in the Table 3. The analysis of the data revealed that the addition of the inhibitor increases the activation enthalpy as compared with free H_2SO_4 acid. The positive sign of ΔH_a reflects an endothermic process. This suggests that the mild steel dissolution needs more energy in the presence of the inhibiter extract [46, 47]. Also, the entropy of activation ΔS, became less negative with the addition of the inhibitor. This indicates an ordered arrangement of Gbj extract compound on the metal surface. This validates the activated complex as an association step rather than a dissociation step, in the rate determining step [47, 48]. Furthermore, the values of E_a obtained for XC48 steel in sulfuric acid solution containing inhibitor are greater with respect to those retrieved for the blank system, this pattern is likely to be related to the formation of a protective adsorbed film on the metallic surface of the working electrode [49].

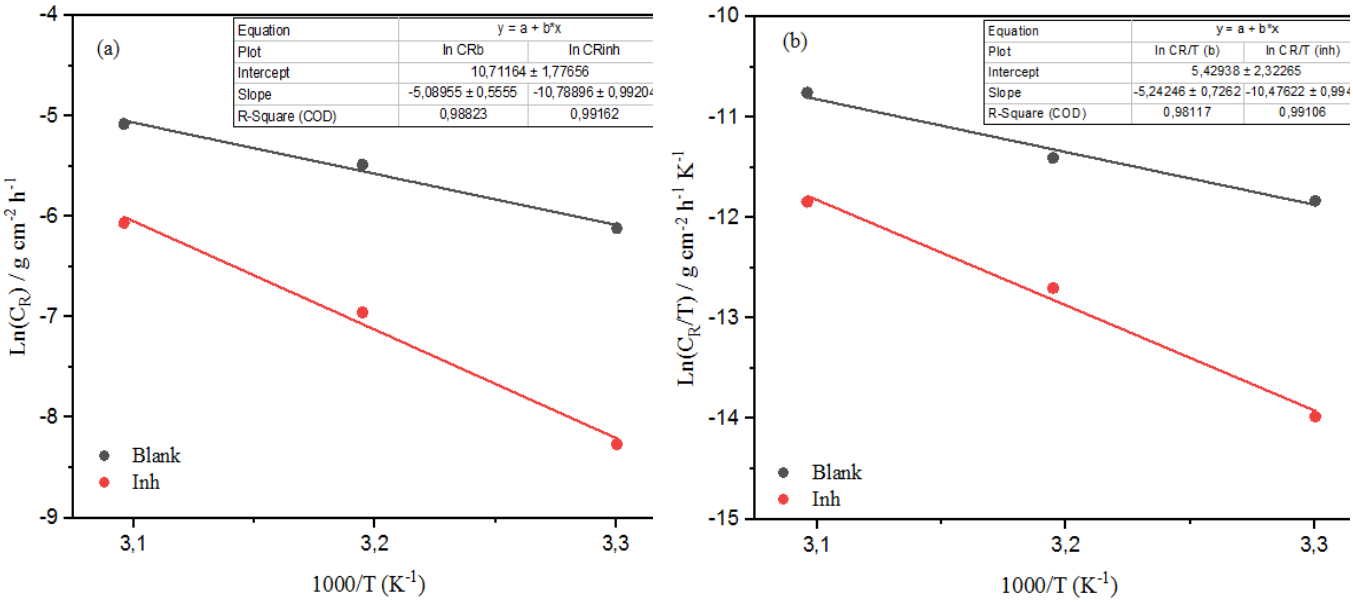

Figure 1. Arrhenius plots of ln(C_R) (a) and Transition state plots of ln(C_R/T) (b) vs 1/T for XC48 mild steel in 0.5 M H_2SO_4 in the absence and presence of optimum concentration (1500 ppm) of Gbj extract.

Table 3. Thermodynamic and activation parameters of XC48 steel in the presence of Gbj extract at different concentration in 0.5 M H_2SO_4 solution. A blank system (without inhibitor) was included as reference.

Parameter	E_a **(kJ·mol^{-1})**	ΔH_a **(kJ·mol^{-1})**	ΔS_a **(J·mol^{-1}·K^{-1})**	ΔG_a **(kJ·mol^{-1})**		
Blank	76.60	70.52	−445.25	308	318	333
1500 ppm	169.76	163.68	−176.59	−19.36	−11.87	−7.08

3.4. Adsorption isotherm

The initial phase of any metal corrosion inhibition is the displacement of water molecules by the adsorbed organic inhibitor molecules at the metal-solution boundary [50, 51]. The adsorption isotherms describe the molecular interactions of the inhibitor molecules with the active sites on the metal surface [52, 53] and provide more insights into the mechanism of corrosion inhibition. Three adsorption models, namely; Langmuir, Freundlich, and Temkin were fitted/tested in this study, to understand the type of reactions that happening on the metal surface. Equations (7), (8) and (9) represent the Langmuir, Freundlich and Temkin adsorption isotherms respectively.

$$\frac{\theta}{1-\theta} = C_{\text{inh}} + K_{\text{ads}} \tag{7}$$

$$\log\theta = \log K_{\text{ads}} + \frac{1}{n}\log C_{\text{inh}} \tag{8}$$

$$\theta = \frac{-1}{2a}\ln K_{ads} + \frac{-1}{2a}C_{inh} \quad (9)$$

where θ is the surface coverage, C_{inh} is the inhibitor concentration, K_{ads} represents the equilibrium adsorption coefficient, α is a sign dependent molecular interaction parameter and *n* signifies an exponent characteristic of the type of adsorbate. The Langmuir adsorption isotherm (Figure 2) was found to provide the best description of the behavior of the investigated inhibitor extract with near unity correlation coefficient (R^2) value, see Table 4.

Table 4. Correlation coefficients (R^2) obtained by the different isotherms for mild steel XC48 in 0.5 M H_2SO_4 solution at different inhibitor concentrations.

Langmuir isotherm	Temkin isotherm	Frumkin isotherm
$R^2 = 0.9976$	$R^2 = 0.9616$	$R^2 = 0.8972$

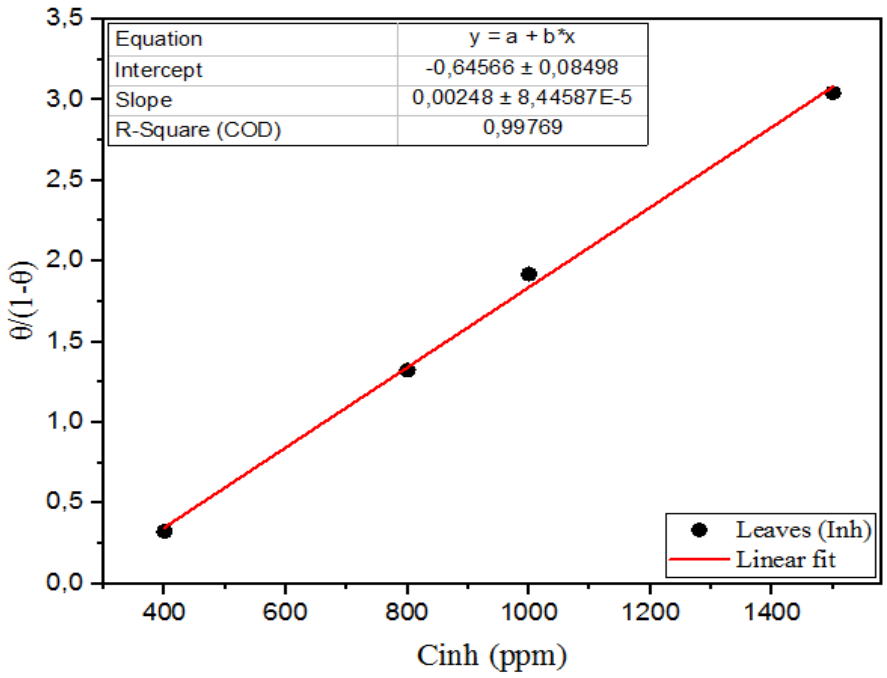

Figure 2. Langmuir isotherm for adsorption of Gbj leaves on XC48 mild steel surface in 0.5 M H_2SO_4 solution.

The equilibrium constant *K* and adsorption free energy (ΔG_{ads}) can be related using the Equation (10) [54].

$$\Delta G_{ads} = -RT\ln 55.5K \quad (10)$$

where *R* is global gas constant and *T* is the absolute temperature (298 K), and 55.55 mol·l^{-1} is the water molar concentration in the liquid phase. The value ΔG_{ads} less than −20 kJ/mol defines physical adsorption mode (adsorption due to electrostatic interaction between charged metal surface and charged inhibitor species) while value around −40 kJ/mol is

consistent with chemical adsorption mode (adsorption that involves electron sharing or transfer from inhibitor molecules to empty orbital of metal). ΔG_{ads} value in between the defined boundaries for physisorption and chemisorption is always associated with mixed adsorption (both chemisorption and physisorption) [55, 56]. The calculated ΔG_{ads} values reported in Table 3 were less than −20 kJ/mol, this confirm that *Grewia bicolor* Juss extract adsorption on XC48 mild steel surface is typical of physisorption.

3.5. Electrochemical measurements

3.5.1. OCP

To understand the influence of the methanolic extract concentration of *Grewia bicolor* Juss leaves, which is used as a corrosion inhibitor of XC48 steel in H_2S0_4 medium (0.5 M), we have started with the Open Circuit Potential Figure 3, to giving information about the evolution of the corrosion potential (E_{corr}) as a function of the immersion time for different inhibitor concentrations. We note that the evolution of the potential over time illustrates that for all concentrations the potential first becomes negative (anodic) then tends towards more positive values followed by a stabilization step, the change of OCP with time measurements thus indicated that the presence of *Grewia bicolor* Juss leaves extract decreases the aggressiveness action of H_2SO_4 by shifting its potential in the less negative direction and this effect was found to increase with increase of the concentration of *Grewia bicolor* Juss leaves extract [33].

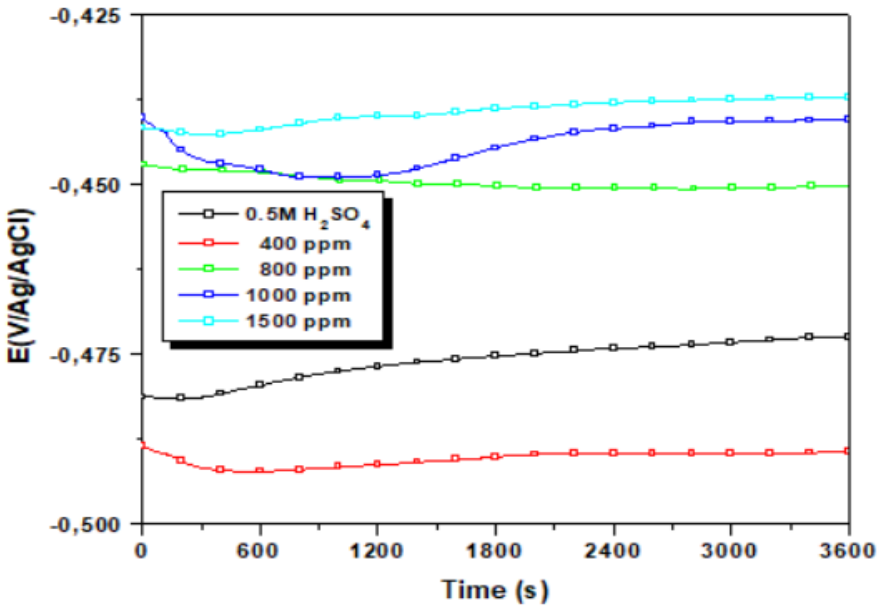

Figure 3. Open circuit potential *versus* time of XC48 steel exposed to 0.5 M H_2SO_4 solution containing different concentrations of *Grewia bicolor* Juss leaves extract.

3.5.2. Tafel polarization

The potential of the electrode is stabilized for 60 min before proceeding to the measurements of the curves $I=f(E)$ at room temperature, Figure 4 shows the curves of cathodic and anodic polarization of XC48 steel in H_2SO_4 medium (0.5 M), in the absence and presence of different concentrations of the inhibitor. The values of inhibition efficiency, calculated from Equation (3).

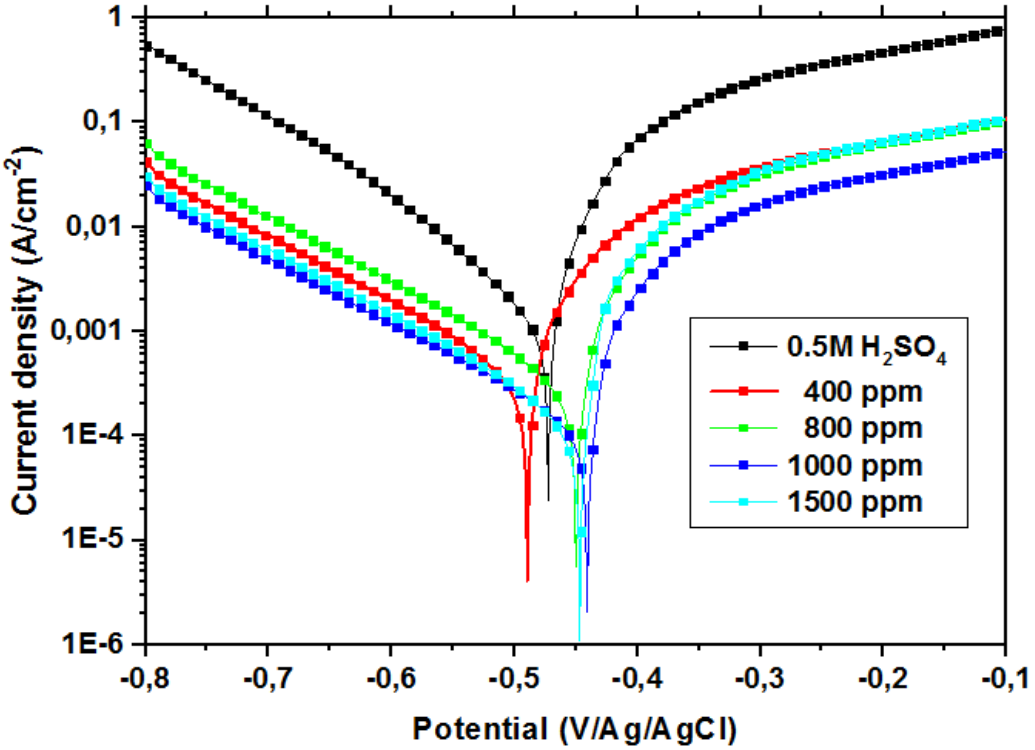

Figure 4. Polarization curves of XC48 steel in H_2SO_4 medium (0.5 M) without and with different concentrations of *Grewia bicolor* Juss leaves extract at 298 K.

The corrosion parameters such as corrosion current (I_{corr}), corrosion potential (E_{corr}), cathodic (β_c) and anodic (β_a) Tafel slopes were calculated by extrapolating the Tafel plot and tabulating in Table 5, which organizes the values of electrochemical parameters from the cathode and anode curves as well as the corresponding inhibitory efficiency (*IE*) at each concentration. It shows that *IE* values increase with an increase in the *Grewia bicolor* Juss leaves extract concentration, however, the I_{corr} value decrease as the *Grewia bicolor* Juss leaves extract concentration increases, reaching its lowest value with the addition of 1500 ppm solution. Both, the cathodic and anodic Tafel slopes, were affected by the presence of *Grewia bicolor* Juss leaves extract; even so, the corrosion potential changed considerably comparing to that of the blank, with a range of −22.082 to 18.995 mV. According to the literature [57–61], if the displacement in corrosion potential is more than 85 mV with respect to corrosion potential of the blank, the inhibitor can be seen as a cathodic or anodic type. In

our case the maximum displacement was 18.995 mV, which indicated that the *Grewia bicolor* Juss leaves extract can be classed as mixed-type inhibitor.

Table 5. Electrochemical parameters calculated from polarization measurement on the XC48 steel in the absence and presence of the different concentrations of *Grewia bicolor* Juss leaves extract at 298 K.

***C* (ppm)**	**E_{corr} (mV)**	**I_{corr} (μA)**	**β_c (mV)**	**β_a (mV)**	**R_p (Ω)**	**%*IE***	**θ**
Blank	−472.4	1208.97	−113.53	34.55	17.86		
400	−489.3	296.225	−120.00	27.39	52.09	75.50	0.7550
800	−450.03	218.34	−121.35	26.66	68.04	81.94	0.8194
1000	−440.52	93.94	−118.58	19.97	111.15	92.23	0.9223
1500	−447	81.36	−98.27	18.62	122.77	93.27	0.9327

3.5.3. EIS results

The EIS study has been adopted as a well-recognized and generally accepted technique to verify the adsorption process at the metal/electrolyte interface. The recorded spectra were reported in the form of Nyquist diagrams, Bode and phase plots in Figure 5 ((a), (b) and (c) respectively). All impedance spectra in the Nyquist plots Figure 5 (a) for H_2SO_4 medium (0.5 M) without and with inhibitor show a single semicircle with a diameter that increases with increasing inhibitor concentration This means that the corrosion process was controlled by a charge transfer reaction mainly [62] and inhomogeneity of surface created due to the adsorption of the inhibitor molecules on metal surface [63]. The shapes of Nyquist plots are similar that indicate that protection mechanism does not change during the whole process [64, 65]. It can be seen that the magnitude of values of $\log|Z|$ in the Bode modulus together with the phase angle (φ) increase in the presence of the Gbj extract and the effect is monotonic with the inhibitor concentration. Furthermore, all phase-frequency angle plots indicate a single wave, confirming the unique constant obtained by the Nyquist diagrams. According to Akhil Saxena [66] the electrochemical behavior at the steel solution interface is capacitive or resistive, if phase angle equals to 90° or 0°, respectively.

The fitting of the obtained impedance diagrams was done according to equivalent circuit depicted in Figure 6. The various impedance parameters such as charge transfer resistance R_{ct}, double layer capacitances C_{dl} and inhibition efficiency (*IE*%) are cited in Table 6. The charge-transfer resistance values are calculated from the difference in impedance at lower and higher frequencies. The double layer capacitance (C_{dl}) and the frequency at which the imaginary component of the impedances is found as represented in Equation (11) [67]:

$$C_{dl} = \left(\frac{1}{\omega \cdot R_{ct}} \right) \tag{11}$$

where $\omega = 2\pi f$.

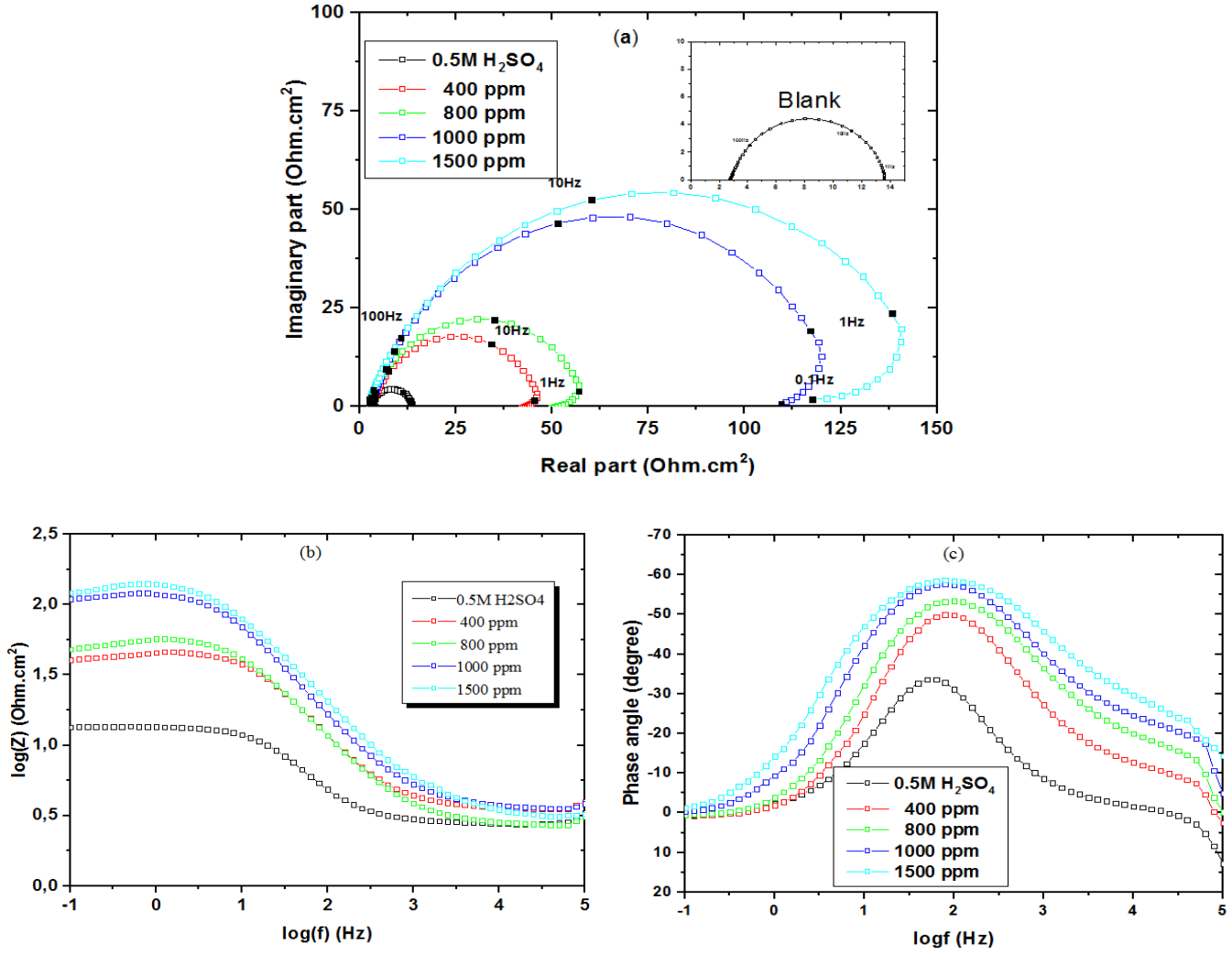

Figure 5. Nyquist (a), Bode (b) and phase angle (c) plots of the corrosion of XC48 steel in 0.5 M H_2SO_4 without and with different concentrations of Gbj extract.

Table 6. EIS parameters for XC48 steel corrosion 0.5 M H_2SO_4 with different concentration of the inhibitor.

***C* (ppm)**	***R*$_s$ (Ω·cm^2)**	***R*$_{ct}$ (Ω·cm^2)**	***C*$_{dl}$ (μF·cm^{-2})**	***E* (%)**
Blank	2.778	10.923	460.76	
400	3.152	44.04	228.02	75.18
800	2.685	56.60	223.36	80.70
1000	3.126	122.61	163.421	91.08
1500	2.710	148.09	135.300	92.62

It can be seen from data in Table 6 that the R_{ct} values significantly increases with the increasing the concentrations of the inhibitors. On the other hand, the values of C_{dl} decreased

with an increase in the inhibitor concentration thus with inhibition efficiencies. This decrease in C_{dl} can result from a decrease in local dielectric constant and an increase in the thickness of the electrical double layer, signifying that molecule inhibitors acts by adsorption at the solution/interface [68, 69].

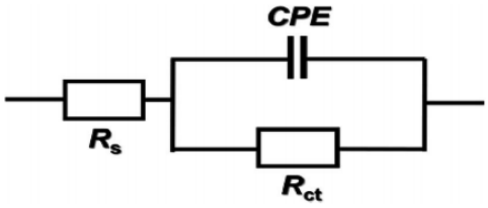

Figure 6. Equivalent electrical circuit used to fit the electrochemical impedance plots.

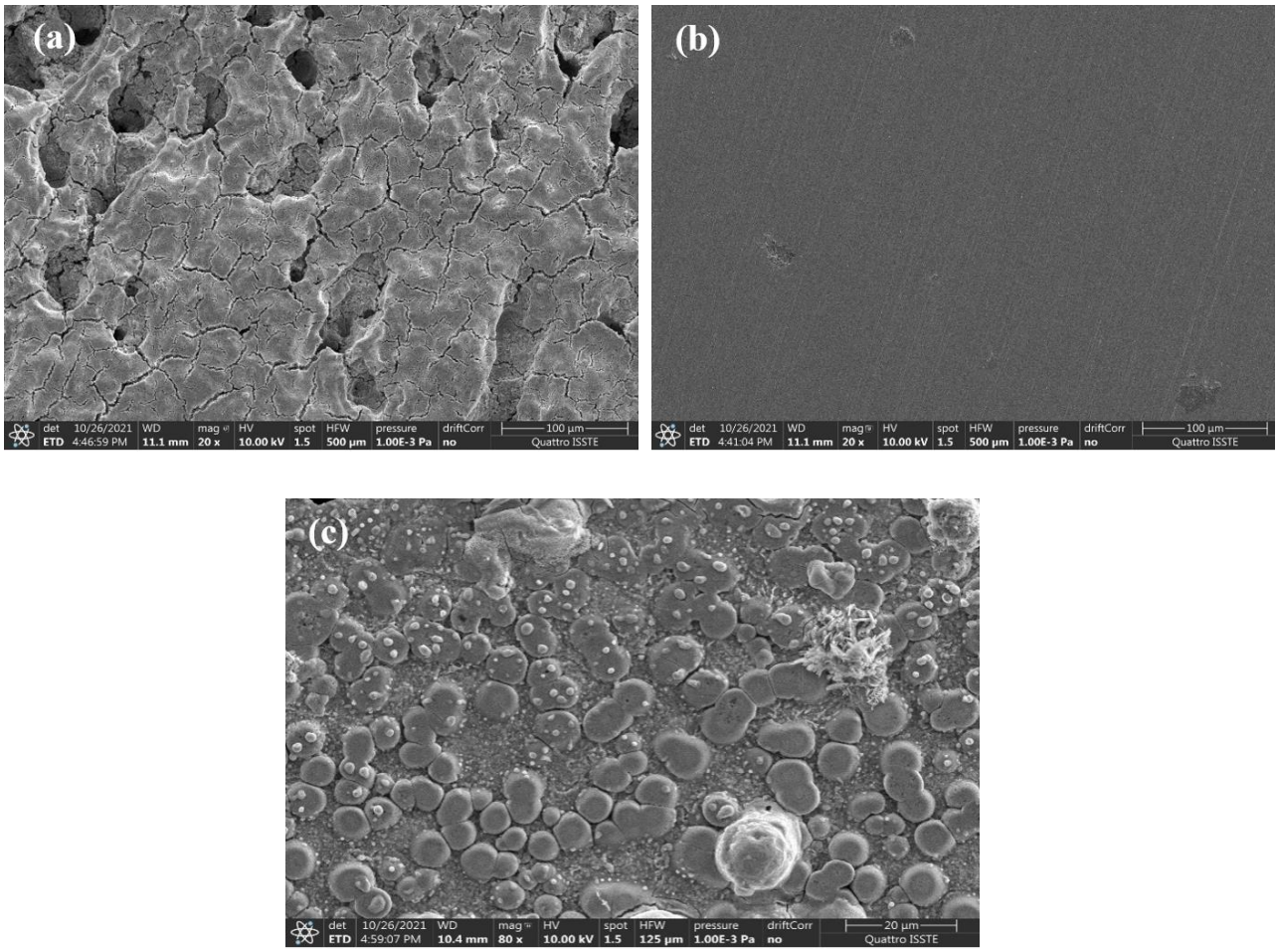

Figure 7. SEM images of XC48 steel surface: (a) polished XC48 steel surface, (b) XC48 steel after 24 h of immersion in 0.5 M H_2SO_4, (c) XC48 steel er 24 h of immersion in 0.5 M H_2SO_4 with 1500 ppm of *Grewia bicolor* Juss extract.

3.6. SEM, EDS analysis

The scanning electron micrographs of the surface morphology of the XC48 steel, after immersion in 0.5 M sulfuric acid solution for 24 h, with and without the optimum concentration (1500 ppm) of Gbj extract are given in Figure 7. Before the immersion, the surface of XC48 steel sample was relatively smooth Figure 7(a). However, in sulfuric acid, XC48 steel is heavily damaged with wide and deep holes, Figure 7(b). But after the exposure to the acid solution with 1500 ppm of Gbj extract Figure 7(c), it can observe that the surface of the working electrode became more heterogeneous and has larger deposits than those observed for the sulfuric acid alone. This difference clearly indicates that the adsorbed extract molecules protect the steel surface of the working electrode. The chemical composition of steel samples immersed in sulfuric solution (Table 7), revealed the presence of elements such as C, F, Mn and Zn. These elements are related to the composition of XC48 meld steel sample. A comparison of Fe, C, Si and Mn percentages before and after sulfuric exposure clearly testify that the metal lost part of its constituent elements due to the corrosion phenomena occurring in the acid medium [33, 71].

Table 7. Elemental composition (quantitative) of XC48 steel surface (Bare) and after 24 h immersion in 0.5 M H_2SO_4 in the presence and absence of the Gbj extract from EDS measurements.

Element (%)	Fe	C	O	F	Si	Mn	Zn	S
Bare XC48 steel	84.25	5.84	–	4.49	0.96	3.30	1.16	–
Blank	51.54	5.64	34.60	0.34	–	1.06	–	5.63
1500 ppm	62.27	6.11	17.37	0.44	0.38	–	–	2.24

3.7. FTIR analysis

The FT-IR analysis of the pure *Grewia bicolor* Juss leaves extract was used to identify the functional groups formed on the surface of the XC48 mild steel to form the protective layer, and are displayed in Figure 8 (a) and (b). The spectra of the pure extract Figure 8 (a) showed the presence of important functional active groups, such as the $-CH_2-$ identified through its asymmetric and symmetric stretching at 2928 cm^{-1} and 2884 cm^{-1}, respectively. The broad peak at 3450 cm^{-1}, associated to the O–H stretching indicates an alcohol/phenol functional group [28, 33]. The sharp band observed at 1662 cm^{-1} indicated the presence of C=O stretching mode [72]. The peak obtained at 1502 cm^{-1} represents the C=C stretching of the aromatic ring, other sharp peak at 878 cm^{-1} can be assigned the presence of C=C [73, 74]. The peaks for C–H scissoring and bending modes can be seen around 1389 cm^{-1} and 1252 cm^{-1} [75]. The peaks observed at 1152 cm^{-1} and 1097 cm^{-1} are due to the C–O stretching region resulting from stretching vibrations of C–O (enol group) and C–O–C (ester group). In the fingerprint region, a peak was seen at 1252 cm^{-1} that is characteristic to phenols [33]. The Fourier transform infrared spectrum of adsorbed protective layer formed on the surface of XC48 steel after immersion in 0.5 M H_2SO_4 containing optimum

concentration (1500 ppm) of *Grewia bicolor* Juss extract was reported in Figure 8 (b). It could be seen that certain peaks were significantly reduced compared to the Figure 8 (a). The absorption bands at 3408 cm^{-1}, 1641 cm^{-1}, and 1096 cm^{-1} were related to the O–H, C=O and C–O stretching modes respectively. The intense peak around 615 cm^{-1} corresponds to the stretching of aromatic carbon [72]. These results show that the important role played by the oxygen atoms and aromatic rings in the process of adsorption.

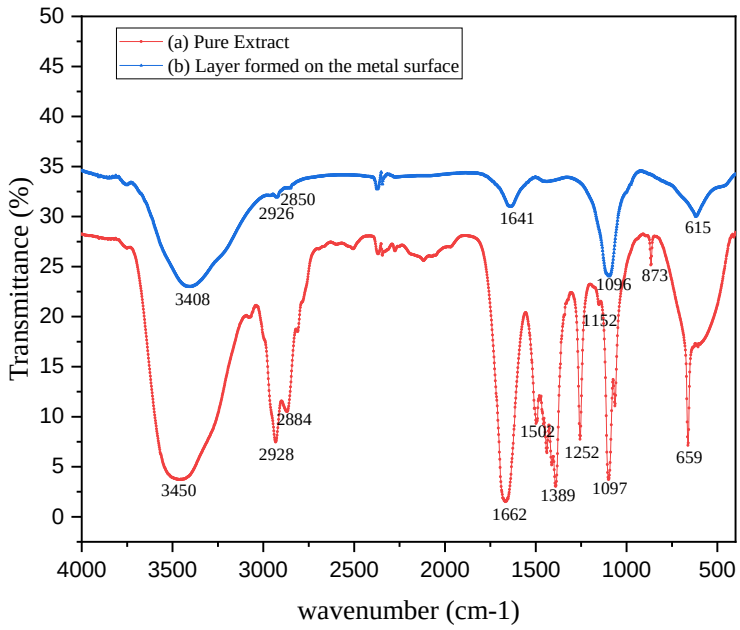

Figure 8. FT-IR spectra of (a) *Grewia bicolor* Juss leaf extract (b) adsorbed layer formed on the surface of XC48 steel after immersion in 0.5 M H_2SO_4 containing inhibitors.

Conclusion

Grewia bicolor Juss leaves extract has been evaluated as a corrosion inhibitor for XC48 steel in 0.5 M H_2SO_4. The extract of Gbj leaves acted as a mixed inhibitor for XC48 steel in 0.5 M H_2SO_4 solution. The inhibition efficiency rises with increasing concentration of Gbj leaves with the highest inhibition efficiency being 93.27% for 1500 ppm. Gravimetric measurements realized are in good agreement with the values obtained from the Electrochemical measurements with a maximum *IE* of 88.63 % at 24 hours. The effect of temperature on the inhibition efficiency at this concentration (1500 ppm), was also studied at different temperatures, ranging from 298 K to 333 K by weight loss measurements. The inhibition efficiency decreases, in opposite, the corrosion rate raises in higher temperature. The activation and free energy values of the inhibition reaction supported the hypothesis of a physisorption mechanism a process well described by the Langmuir equilibrium mode. Also, EIS measurements showed the increase in corrosion resistance offered by Gbj when increasing their concentration in the corrosive solution. Surface analyses by SEM/EDS and

FT-IR confirmed the presence of a protective film made up Gbj extract molecules on the metallic surface.

References

1. N. M'hiri, D. Veys-Renaux, E. Rocca, I. Ioannoua, N.M. Boudhrioua and M. Ghoul, Corrosion inhibition of carbon steel in acidic medium by orange peel extract and its main antioxidant compounds, *Corros. Sci*., 2016, **102**, 55–62. doi: 10.1016/j.corsci.2015.09.017
2. P.E. Alvarez, M.V. Fiori-Bimbi, A. Neske, S.A Brandan and C.A Gervasi, *Rollinia occidentalis* extract as green corrosion inhibitor for carbon steel in HCl solution, *J. Ind. Eng. Chem*., 2018, **58**, 92–99. doi: 10.1016/j.jiec.2017.09.012
3. M. Tezeghdenti, L. Dhouibi and N. Etteyeb, Corrosion inhibition of carbon steel in 1 M sulphuric acid solution by extract of *Eucalyptus globulus* leaves cultivated in Tunisia arid zones, *J. Bio- Tribo-Corros*., 2015, **1**, 16. doi: 10.1007/s40735-015-0016-x
4. N.A. Negm, N.G. Kandile, E.A. Badr and M.A. Mohammed, Gravimetric and electrochemical evaluation of environmentally friendly nonionic corrosion inhibitors for carbon steel in 1 M HCl, *Corros. Sci*., 2012, **65**, 94–103. doi: 10.1016/j.corsci.2012.08.002
5. A. Lecante, F. Robert, P.A. Blandinières and C. Roos, Anti-corrosive properties of *S. tinctoria* and *G. ouregou* alkaloid extracts on low carbon steel, *Current Applied Physics*, 2011, **11,** no. 3, 714–724. doi: 10.1016/j.cap.2010.11.038
6. F. Bentiss, M. Lagrenee, M. Traisnel and J.C. Hornez, The corrosion inhibition of mild steel in acidic media by a new triazole derivative, *Corros. Sci*., 1999, **41**, no. 4, 789–803. doi: 10.1016/S0010-938X(98)00153-X
7. M. Mobin and M. Rizvi, Polysaccharide from *Plantago* as a green corrosion inhibitor for carbon steel in 1 M HCl solution, *Carbohydr. Polym*., 2017, **160**, 172–183. doi: 10.1016/j.carbpol.2016.12.056
8. X. Wang, H. Yang and F. Wang, An investigation of benzimidazole derivative as corrosion inhibitor for mild steel in different concentration HCl solutions, *Corros. Sci*., 2011, **53**, no. 1, 113–121. doi: 10.1016/j.corsci.2010.09.029
9. A. Khadraoui, A. Khelifa, M. Hadjmeliani, R. Mehdaoui, K. Hachama, A. Tidu, Z. Azari, I.B. Obot and A. Zarrouk, Extraction, characterization and anti-corrosion activity of *Mentha pulegium* oil: Weight loss, electrochemical, thermodynamic and surface studies, *J. Mol. Liq*., 2016, **216**, 724–731. doi: 10.1016/j.molliq.2016.02.005
10. A. Sedik, D. Lerari, A. Salci, S. Athmani, K. Bachari, İ.H. Gecibesler and R. Solmaz, Dardagan Fruit extract as eco-friendly corrosion inhibitor for mild steel in 1 M HCl: Electrochemical and surface morphological studies, *J. Taiwan Inst. Chem. Eng*., 2020, **107**, 189–200. doi: 10.1016/j.jtice.2019.12.006
11. N.K. Gupta, P.G. Joshi, V. Srivastava and M.A. Quraishi, Chitosan: a macromolecule as green corrosion inhibitor for mild steel in sulfamic acid useful for sugar industry, *Int. J. Biol. Macromol*., 2018, **106**, 704–711. doi: 10.1016/j.ijbiomac.2017.08.064

12. P. Parthipan, J. Narenkumar, P. Elumalai, P.S. Preethi, A.U.R. Nanthini, A. Agrawal and A. Rajasekar, Neem extract as a green inhibitor for microbiologically influenced corrosion of carbon steel API 5LX in a hyper saline environment, *J. Mol. Liq.*, 2017, **240**, 121–127. doi: 10.1016/j.molliq.2017.05.059
13. C. Verma, E.E. Ebenso, I. Bahadur and M.A. Quraishi, An overview on plant extracts as environmental sustainable and green corrosion inhibitors for metals and alloys in aggressive corrosive media, *J. Mol. Liq.*, 2018, **266**, 577–590. doi: 10.1016/j.molliq.2018.06.110
14. M. Sohail, F. Hussain, A.D. Chandio and M. Sheikh, High temperature effectiveness of ginger extract as green inhibitor for corrosion in mild steel, *NUST Journal of Engineering Sciences*, 2018, **11**, no. 1, 26–32. doi: 10.24949/njes.v11i1.266
15. E. Topal and G. Gece, A theoretical study on chemically elegant proton pump inhibitors in search of novel green corrosion inhibitors, *Prot. Met. Phys. Chem. Surf.*, 2017, **53**, 1173–1180. doi: 10.1134/S2070205118010288
16. A. Belakhdar, H. Ferkous, S. Djellali, R. Sahraoui, H. Lahbib, B.Y. Amor and S. Djellali, Corrosion inhibition performance of Rosmarinus officinalis methanolic extract on carbon steel XC48 in acidic medium (2M HCl), *Mater. Biomater. Sci.*, 2020, **3**, 46–53.
17. B. Sanyal, Organic compounds as corrosion inhibitors in different environments – A review, *Prog. Org. Coat.*, 1981, **9**, no. 2, 165–236. doi: 10.1016/0033-0655(81)80009-X
18. A. Miralrio and A.E. Vázquez, Plant Extracts as Green Corrosion Inhibitors for Different Metal Surfaces and Corrosive Media: A Review, *Processes*, 2020, **8**, no. 8, 942. doi: 10.3390/pr8080942
19. M.H. Hussin, M.J. Kassim, N.N. Razali, N.H. Dahon and D. Nasshorudin, The effect of *Tinospora crispa* extracts as a natural mild steel corrosion inhibitor in 1 M HCl solution, *Arabian J. Chem.*, 2016, **9**, 616–624. doi: 10.1016/j.arabjc.2011.07.002
20. M.H. Hussin, M.J. Kassim, The corrosion inhibition and adsorption behavior of *Uncaria gambir* extract on mild steel in 1 M HCl, *Mater. Chem. Phys.*, 2011, **125**, no. 3, 461–468. doi: 10.1016/j.matchemphys.2010.10.032
21. H. Hassannejad and A. Nouri, Sunflower seed hull extract as a novel green corrosion inhibitor for mild steel in HCl solution, *J. Mol. Liq.*, 2018, **254**, 377–382. doi: 10.1016/j.molliq.2018.01.142
22. A. Jmiai, B. El Ibrahimi, A. Tara, M. Chadili, S. El Issami, O. Jbara, A. Khallaayoun and L. Bazzi, Application of *Zizyphus Lotuse*-pulp of Jujube extract as green and promising corrosion inhibitor for copper in acidic medium, *J. M. Liq.*, 2018, **268**, 102–113. doi: 10.1016/j.molliq.2018.06.091
23. A. Khadraoui, A. Khelifa, K. Hachama and R. Mehdaoui, *Thymus algeriensis* extract as a new eco-friendly corrosion inhibitor for 2024 aluminium alloy in 1 M HCl medium, *J. Mol. Liq.*, 2016, **214**, 293–297. doi: 10.1016/j.molliq.2015.12.064

24. K.H. Hassan, A.A. Khadom and N.H. Kurshed, *Citrus aurantium* leaves extracts as a sustainable corrosion inhibitor of mild steel in sulfuric acid, *S. Afr. J. Chem. Eng*., 2016, **22**, 1–5. doi: 10.1016/j.sajce.2016.07.002
25. O.O. Dominic and O. Monday, Optimization of the inhibition efficiency of mango extract as corrosion inhibitor of mild steel in 1.0 M H_2SO_4 using response surface methodology, *J. Chem. Technol. Metall*., 2016, **51**, no. 1, 302–314.
26. R.T. Loto, Surface coverage and corrosion inhibition effect of *Rosmarinus officinalis* and zinc oxide on the electrochemical performance of low carbon steel in dilute acid solutions, *Results Phys*., 2018, **8**, 172–179. doi: 10.1016/j.rinp.2017.12.003
27. F. Bouhlal, N. Labjar, F. Abdoun, A. Mazkour, M, Serghini-Idrissi, M. El Mahi, El M. Lotfi, A. Skalli and S. El Hajjaji, Chemical and electrochemical studies of the inhibition performance of hydro-alcoholic extract of used coffee grounds (HECG) for the corrosion of C38 steel in 1 M hydrochloric acid, *Egypt. J. Pet*., 2020, **29**, no. 1, 45–52. doi: 10.1016/j.ejpe.2019.10.003
28. H. Lahbib, S.B. Hassen, H. Gerengi, M. Rizvi and Y.B. Amor, Corrosion inhibition performance of dwarf palm and *Cynara cardunculus* leaves extract for St37 steel in 15% H_2SO_4: a comparative study, *J. Adhes. Sci. Technol*., 2020, **35**, no. 7, 691–722. doi: 10.1080/01694243.2020.1819701
29. N. Chafai, S. Chafaa, K. Benbouguerra, D. Daoud, A. Hellal and M. Mehri, Synthesis, characterization and the inhibition activity of a new α-aminophosphonic derivative on the corrosion of XC48 carbon steel in 0.5 M H_2SO_4: Experimental and theoretical studies, *J. Taiwan Inst. Chem. Eng*., 2017, **70**, 331–344. doi: 10.1016/j.jtice.2016.10.026
30. G. Ghosh, P. Panda, M. Rath, A. Pal, T. Sharma and D. Debajyoti, GC-MS analysis of bioactive compounds in the methanol extract of *Clerodendrum viscosum* leaves, *Pharmacogn. Res*., 2015, **7**, no. 1, 110–113. doi: 10.4103/0974-8490.147223
31. M.A. Deyab, K. Eddahaoui, R. Essehli, T. Rhadfi, S. Benmokhtar and G. Mele, Experimental evaluation of new inorganic phosphites as corrosion inhibitors for carbon steel in saline water from oil source wells, *Desalination*, 2016, **383**, 38–45. doi: 10.1016/j.desal.2016.01.019
32. A. Zarrouk, H. Zarrok, Y. Ramli, M. Bouachrine, B. Hammouti, A. Sahibed-dine and F. Bentiss, Inhibitive properties, adsorption and theoretical study of 3,7-dimethyl-1(prop-2-yn-1-yl)quinoxalin-2(1H)-one as efficient corrosion inhibitor for carbon steel in hydrochloric acid solution, *J. Mol. Liq*., 2016, **222**, 239–252. doi: 10.1016/j.molliq.2016.07.046
33. W. Ebdelly, S. Ben Hassen, X.R. Novoa and Y. Ben Amor, Inhibition of carbon steel corrosion in neutral calcareous synthetic water by *Eruca sativa* extract, *Prot. Met. Phys. Chem. Surf*., 2019, **55**, no. 3, 591–602. doi: 10.1134/S2070205119030110
34. N.A. Negm, N.G. Kandile, E.A. Badr and M.A. Mohamed, Gravimetric and electrochemical evaluation of environmentally friendly nonionic corrosion inhibitors for carbon steel in 1 M HCl, *Corros. Sci*., 2012, **65**, 94–103. doi: 10.1016/j.corsci.2012.08.002

35. H.M. Abd El-Lateef, M.A. Abo-Riya and A.H. Tantawy, Empirical and quantum chemical studies on the corrosion inhibition performance of some novel synthesized cationic gemini surfactants on carbon steel pipelines in acid pickling processes, *Corros. Sci*., 2016, **108**, 94–110. doi: 10.1016/j.corsci.2016.03.004
36. F. Ivušić, O. Lahodny-Šarc, H.O. Ćurković and V. Alar, Synergistic inhibition of carbon steel corrosion in seawater by cerium chloride and sodium gluconate, *Corros. Sci*., 2015, **98**, 88–97. doi: 10.1016/j.corsci.2015.05.017
37. F.El-Taib Heakal, A.S. Fouda and S.S Zahran, environmentally safe protection of carbon steel corrosion in sulfuric acid by thiouracil compounds, *Int. J. Electrochem. Sci*., 2015, **10**, no. 2, 1595–1615.
38. H. Gerengi, H.I. Ugras, M.M. Solomon, A.S. Umoren, M. Kurtay and N. Atar, Synergistic corrosion inhibition effect of 1-ethyl-1-methylpyrrolidinium tetrafluoroborate and iodide ions for low carbon steel in HCl solution, *J. Adhes. Sci. Technol*., 2016, **30**, no. 21, 2383–2403. doi: 10.1080/01694243.2016.1183407
39. H. Gerengi, I. Uygur, M. Solomon, M. Yildiz and H. Goksu, Evaluation of the inhibitive effect of *Diospyros kaki* (Persimmon) leaves extract on St37 steel corrosion in acid medium, *Sustainable Chem. Pharm*., 2016, **4**, 57–66. doi: 10.1016/j.scp.2016.10.003
40. M. Tezeghdenti, L. Dhouibi and N. Etteyeb, Corrosion inhibition of carbon steel in 1 M sulphuric acid solution by extract of *Eucalyptus globulus* leaves cultivated in Tunisia arid zones, *J. Bio-and Tribo-Corrosion*, 2015, **1**, 16. doi: 10.1007/s40735-015-0016-x
41. H. Derfouf, Y. Harek, L. Larabi, W.J. Basirun and M. Ladan, Corrosion inhibition activity of carbon steel in 1.0 M hydrochloric acid medium using *Hammada scoparia* extract: gravimetric and electrochemical study, *J. Adhes. Sci. Technol*., 2019, **33**, no. 8, 808–833. doi: 10.1080/01694243.2018.1562321
42. P. Sakunthala, S.S Vivekananthan, M. Gopiraman, N. Sulochana and A.R. Vincent, Spectroscopic investigations of physicochemical interactions on mild steel in an acidic medium by environmentally friendly green inhibitors, *J. Surfactants Deterg*., 2013, **16**, no. 2, 251–263. doi: 10.1007/s11743-012-1405-5
43. M. Yildiz, H. Gerengi, M.M. Solomon, E. Kaya and S.A. Umoren, Influence of 1-butyl-1-methylpiperidinium tetrafluoroborate on St37 steel dissolution behavior in HCl environment, *Chem. Eng. Commun*., 2018, **205**, no. 4, 538–548. doi: 10.1080/00986445.2017.1407759
44. T. Peme, L.O. Olasunkanmi, I. Bahadur, A.S. Adekunle, M.M. Kabanda and E.E. Ebenso, Adsorption and Corrosion Inhibition Studies of Some Selected Dyes as Corrosion Inhibitors for Mild Steel in Acidic Medium: Gravimetric, Electrochemical, Quantum Chemical Studies and Synergistic Effect with Iodide Ions, *Molecules*, 2015, **20**, no. 9, 16004–16029. doi: 10.3390/molecules200916004
45. C. Verma, M.A. Quraishi, E.E. Ebenso, I.B. Obot and A. El Assyry, 3-Amino alkylated indoles as corrosion inhibitors for mild steel in 1 M HCl: Experimental and theoretical studies, *J. Mol. Liq*., 2016, **219**, 647–660. doi: 10.1016/j.molliq.2016.04.024

46. G.M. Al-Senani and M. Alshabanat, Study the corrosion inhibition of carbon steel in 1 M HCl using extracts of date palm waste, *Int. J. Electrochem. Sci*., 2018, **13**, no. 4, 3777–3788. doi: 10.20964/2018.04.03
47. S.S. Shivakumar and K.N. Mohana, Studies on the inhibitive performance of *Cinnamomum zeylanicum* extracts on the corrosion of mild steel in hydrochloric acid and sulphuric acid media, *J. Mater. Environ. Sci*., 2013, **4**, no. 3, 448–459.
48. A. Hamdy and N.Sh. El-Gendy, Thermodynamic, adsorption and electrochemical studies for corrosion inhibition of carbon steel by henna extract in acid medium, *Egypt. J. Pet*., 2013, **22**, no. 1, 17–25. doi: 10.1016/j.ejpe.2012.06.002
49. T.K. Bhuvaneswari, V.S. Vasantha and C. Jeyaprabha, Pongamia Pinnata as a green corrosion inhibitor for mild steel in 1N sulfuric acid medium, *Silicon*, 2018, **10**, 1793–1807. doi: 10.1007/s12633-017-9673-3
50. C. Verma, L.O. Olasunkanmi, E.E. Ebenso, M.A. Quraishi and I.B. Obot, Adsorption behavior of glucosamine-based, pyrimidine-fused heterocycles as green corrosion inhibitors for mild steel: experimental and theoretical studies, *J. Phys. Chem. C*, 2016, **120**, no. 21, 11598–11611. doi: 10.1021/acs.jpcc.6b04429
51. N.B. Iroha and L.A. Nanna, Electrochemical and adsorption study of the anticorrosion behavior of Cefepime on Pipeline steel surface in acidic solution, *J. Mater. Environ. Sci*., 2019, **10**, no. 10, 898–908.
52. K.Z. Mohammed, A. Hamdy, A. Abdel-wahab and N.A. Farid, Temperature effect on corrosion inhibition of carbon steel in formation water by non-ionic inhibitor and synergistic influence of halide ions, *Life Sci. J*., 2012, **9**, no. 2, 424–434.
53. M. Behpour, S.M. Ghoreishi, N. Soltani, M. Salavati-Niasari, M. Hamadanian and A. Gandomi, Electrochemical and theoretical investigation on the corrosion of mild steel by thiosalicylaldehyde derivatives in hydrochloric acid solution, *Corros. Sci*., 2008, **50**, no. 8, 2172–2181. doi: 10.1016/j.corsci.2008.06.020
54. H. Lgaz, S. Masroor, M. Chafiq, M. Damej, A. Brahmia, R. Salghi, M. Benmessaoud, I.H. Ali, M.M. Alghamdi, A. Chaouiki and I.-M. Chung, Evaluation of 2-mercaptobenzimidazole derivatives as corrosion inhibitors for mild steel in hydrochloric acid, *Metals*, 2020, **10**, no. 3, 357. doi: 10.3390/met10030357
55. M.M. Solomon and S.A. Umoren, Performance evaluation of poly (methacrylic acid) as corrosion inhibitor in the presence of iodide ions for mild steel in H_2SO_4 solution, *J. Adhes. Sci. Technol*., 2015, **29**, no. 11, 1060–1080. doi: 10.1080/01694243.2015.1017436
56. M.M. Solomon and S.A. Umoren, In-situ preparation, characterization and anticorrosion property of polypropylene glycol/silver nanoparticles composite for mild steel corrosion in acid solution, *J. Colloid Interface Sci*., 2016, **462**, 29–41. doi: 10.1016/j.jcis.2015.09.057
57. S. Tao and H. Huang, Study on Corrosion Inhibition Performance of 1,2-Dithiolane-3-pentanoicacid on X65 Steel in 0.5 M Sulfuric Acid, *Int. J. Electrochem. Sci*., 2019, **14**, no. 6, 5435–5447. doi: 10.20964/2019.06.68

58. M. Pourriahi, M. Nasr-Esfahani and A. Motalebi, Effect of henna and rosemary extracts on the corrosion of 304L stainless steel in 3.5% NaCl solution, *Surface Engineering and Applied Electrochemistry*, 2014, **50**, no. 6, 525–533. doi: 10.3103/S1068375514060088
59. A.K. Satapathy, G. Gunasekaran, S.C. Sahoo, K. Amit and P.V. Rodrigues, Corrosion inhibition by *Justicia gendarussa* plant extract in hydrochloric acid solution, *Corros. Sci*., 2009, **51**, no. 12, 2848–2856. doi: 10.1016/j.corsci.2009.08.016
60. Y. Yan, W. Li, L. Cai and B. Hou, Electrochemical and quantum chemical study of purines as corrosion inhibitors for mild steel in 1 M HCl solution, *Electrochim. Acta*., 2008, **53**, no. 20, 5953–5960. doi: 10.1016/j.electacta.2008.03.065
61. W. Li, Q. He, S. Zhang, C. Pei and B. Hou, Some new triazole derivatives as inhibitors for mild steel corrosion in acidic medium, *J. Appl. Electrochem*., 2008, **38**, 289–295. doi: 10.1007/s10800-007-9437-7
62. K. Shimizu, A. Lasia and J.-F. Boily, Electrochemical impedance study of the hematite/water interface, *Langmuir*, 2012, **28**, no. 20, 7914–7920. doi: 10.1021/la300829c
63. P. Singh and M.A. Quraishi, Corrosion inhibition of mild steel using Novel Bis Schiff's Bases as corrosion inhibitors: Electrochemical and Surface measurement, *Measurement*, 2016, **86**, 114–124. doi: 10.1016/j.measurement.2016.02.052
64. R. Touir, N. Dkhireche, M. Ebn Touhami, M. El Bakri, A.H. Rochdi and R.A. Belakhmima, Study of the mechanism action of sodium gluconate used for the protection of scale and corrosion in cooling water system, *J. Saudi Chem. Soc*., 2014, **18**, no. 6, 873–881. doi: 10.1016/j.jscs.2011.10.020
65. A.K. Singh, B. Chugh, S.Kr. Saha, P. Banerjee, E.E. Ebenso, S. Thakur and B. Pani, Evaluation of anti-corrosion performance of an expired semi synthetic antibiotic cefdinir for mild steel in 1 M HCl medium: An experimental and theoretical study, *Results Phys*., 2019, **14**, 102383. doi: 10.1016/j.rinp.2019.102383
66. A. Saxena, D. Prasad, R. Haldhar, G. Singh and A. Kumar, Use of *Saraca ashoka* extract as green corrosion inhibitor for mild steel in 0.5 M H_2SO_4, *J. Mol. Liq*., 2018, **258**, 89–97. doi: 10.1016/j.molliq.2018.02.104
67. H. Elmsellem, H. Nacer, F. Halaimia, A. Aouniti, I. Lakehal, A. Chetouani, S.S. Al-Deyab, I. Warad, R. Touzani and B. Hammouti, Anti-corrosive properties and quantum chemical study of (E)-4-methoxy-N-(methoxybenzylidene)aniline and (E)-N-(4-methoxybenzylidene)-4-nitroaniline coating on mild steel in molar hydrochloric. *Int. J. Electrochem. Sci*., 2014, **9**, 5328–5351. doi: 10.13140/RG.2.1.4505.2326
68. K. Chkirate, K. Azgaou, H. Elmsellem, B. El Ibrahimi, N.K. Sebbar, E.H. Anouar, M. Benmessaoud, S. El Hajjaji and E.M. Essassi, Corrosion inhibition potential of 2-[(5-methylpyrazol-3-yl)methyl]benzimidazole against carbon steel corrosion in 1 M HCl solution: Combining experimental and theoretical studies, *J. Mol. Liq*., 2021, **321**, 114750. doi: 10.1016/j.molliq.2020.114750

69. M. Prabakaran, S.-H. Kim, A. Sasireka, K. Kalaiselvi and I.-M. Chung, *Polygonatum odaratum* extract as an eco-friendly inhibitor for aluminum corrosion in acidic medium. *J. Adhes. Sci. Technol.*, 2018, **32**, no. 18, 2054–2069. doi: 10.1080/01694243.2018.1462947
70. M. Mobin, M. Basik, J. Aslam, Pineapple stem extract (Bromelain) as an environmental friendly novel corrosion inhibitor for low carbon steel in 1 M HCl, *Measurement*, 2019, **134**, 595–605. doi: 10.1016/j.measurement.2018.11.003
71. E.-S.M. Sherif, Corrosion behavior of magnesium in naturally aerated stagnant seawater and 3.5% sodium chloride solutions, *Int. J. Electrochem. Sci*., 2012, **7**, 4235–4249. doi: 10.1016/S1452-3981(23)19534-4
72. P. Muthukrishnan, B. Jeyaprabha and P. Prakash, Mild steel corrosion inhibition by aqueous extract of *Hyptis Suaveolens* leaves, *Int. J. Ind. Chem*., 2014, **5**, 5. doi: 10.1007/s40090-014-0005-9
73. H. Lahbib, S. Ben Hassen, H. Gerengi and Y. Ben Amor, Inhibition effect of *Cynara cardunculus* leaf extract on corrosion of St37 steel immersed in seawater with and without bleach solution, *Chem. Eng. Commun*., 2020, **208**, no. 9, 1260–1278. doi: 10.1080/00986445.2020.1771320
74. R. Haldhar, D. Prasad and A. Saxena, *Myristica fragrans* extract as an eco-friendly corrosion inhibitor for mild steel in 0.5 M H_2SO_4 solution, *J. Environ. Chem. Eng*., 2018, **6**, no. 2, 2290–2301. doi: 10.1016/J.JECE.2018.03.023
75. D.I. Njoku, E.E. Oguzie and Y. Li, Characterization, electrochemical and theoretical study of the anticorrosion properties of *Moringa oleifera* extract, *J. Mol. Liq*., 2017, **237**, 247–256. doi: 10.1016/j.molliq.2017.04.087

♦ ♦ ♦